ンがどの程度脳に影響を及ぼすかは良く分かっていませんが、人によって「男だけども女の子らしいことが好き」「女だけども男らしいことが好き」といったことが、程度の差がありつつも出てくるのです。

一般に男型脳では空間認識や図形処理を司る部位が先に発達しやすいと言われ、この点がいわゆる「男の子っぽい」遊びを生み出すと考えられています。一方で女型脳は言語能力を司る部位が先に発達しやすく、脳全体の連絡網がよく発達すると言われています。そのため、女の子ではいろいろなお話をしたり、まわりをよく見ていることが多いと考えられます。

また、「男の子だから男の子らしい」「女の子だから女の子らしい」行為を社会的に求めている点もあり、そこから外れることで集団から阻害される感じを持たれる現状もあると思われます。親が自然と男の子らしさ、女の子らしさを求めているのかもしれません。

ご心配のように「男の子っぽい」ことは子どもが生まれ持ってきた性格ですから、どちらかの性に偏った行動を求めるのでなく、すなおに良い面を伸ばすように勧めてあげてください。

Q:子どもへの病気の説明について

A:特にCAHの子どもたちは小さな頃から頻繁に病院に通って診察を受け、薬を飲むことが日常となっています。幼稚園や保育園といった集団に属する年代になると、病院に通院し、お薬を飲むことが「どうも特別なことだ」とわかってきます。3歳すぎの「ねえねえ、なんでなんで？」といった疑問を親にぶつけてくる年代になると、特に自分に起こっていることが疑問の主題ともなり、親御さんは答えに窮することになるかもしれません。

子供の頃に正しい知識を教えられ、望ましい体験を積んでいることが、安定した大人になるためには必要だと言われます。誤魔化したり間違ったことで言い逃れるのではなく、そのときの子どもの年齢に応じ、理解できる言葉を使って本当のことを説明するよう心がけましょう。

幼年時期には病気になって治すためにしているということを中心に、学童期になれば病気の内容とその治療内容を中心に、青年期以降には病態も含めて伝えておくことが大事でしょう。

子どもに病気のことを教えるのに病名が大事なのではありません。今、子どもの体に何が起こっていて、どうしなければいけないのか、しなければどうなるのかといった事柄を正しく伝えて行きましょう。

小さな子どもは、親が手本であり、親が常に正しいことを言って行なっていると思っています。それは子どもから親への信頼の証であると言えるでしょう。ですから、親も子どもにしっかり向きあって伝えていくことがとても大事なことなのです。

Q:この病気で使える公費負担制度はありますか。

A:小児慢性特定疾患治療研究事業医療給付が、18歳以後20歳まで延長が可能です。成人以降の公的な給付制度はまだ確立されていません。

## 編集後記

これまでもCAHのご家族から、同じ病気をもつ子どものお父さん、お母さんと話ができないでしょうか、という問い合わせが幾度もありました。私たち医療グループはどのような形で患者さんとご家族のご希望に沿った活動ができるかと幾度も話し合いを重ねました。

その結果、まずは始めることだ、そして続けることだ、と2012年1月から「大阪母子センターCAHの会」を立ち上げたのです。これまで3回、このCAHの会を開き、いろいろの角度から話題を提供し、ご家族の意見もお聞きしました。そのなかでスタッフから、これまで話した内容を判りやすい読みものにしてはどうか、との提案があり作り上げたのがこの小冊子です。内容を読んで頂ければお分かりのように、CAHの子どもさんをもつご家族が抱いておられる心配や疑問にできるだけ答えようと、私たちグループがそれぞれの専門知識を持ち寄り書き上げ、編集しました。

これからも皆様のご意見やご質問、要望をどしどし寄せていただき、さらに版を重ねてより良い冊子が作られることを願っております。

執筆者(五十音順)

位田　忍(大阪府立母子保健総合医療センター　消化器・内分泌科　主任部長)
井上佳世(大阪府立母子保健総合医療センター　遺伝診療科　遺伝カウンセラー)
石見和世(大阪府立母子保健総合医療センター　看護部　小児看護専門看護師)
岡本伸彦(大阪府立母子保健総合医療センター　遺伝診療科　主任部長)
小杉　恵(大阪府立母子保健総合医療センター　子どものこころの診療科　部長)
佐保美奈子(大阪府立大学大学院看護学研究科　准教授)
島田憲次(大阪府立母子保健総合医療センター　泌尿器科　主任部長)
平山　哲(大阪府立母子保健総合医療センター　子どものこころの診療科　医長)

この小冊子は、
平成 25 年度　厚生労働科学研究費補助金　難治性疾患克服研究事業「性分化疾患の実態把握と病態解明ならびに標準的診断・治療指針の作成」（分担研究者：島田憲次）の助成を受けて、企画・製作されました。

CAH の子どもをもつ家族のガイドブック

編集：　島田憲次
発行年月日：　平成 25 年　 3 月　 3 日
印刷：キクイ印刷工芸社　TEL072-956-6881

## 第46回　日本小児内分泌学会学術集会・特別企画

# DSDセミナー in Osaka

*～DSDをめぐる諸問題の解決をめざして～*

開催日時：平成24年9月29日（土）　15：30-17：00
場　　所：大阪国際会議場　10階　1003会場

セミナー事務局長：大阪府立母子保健総合医療センター
消化器内分泌科　位田忍

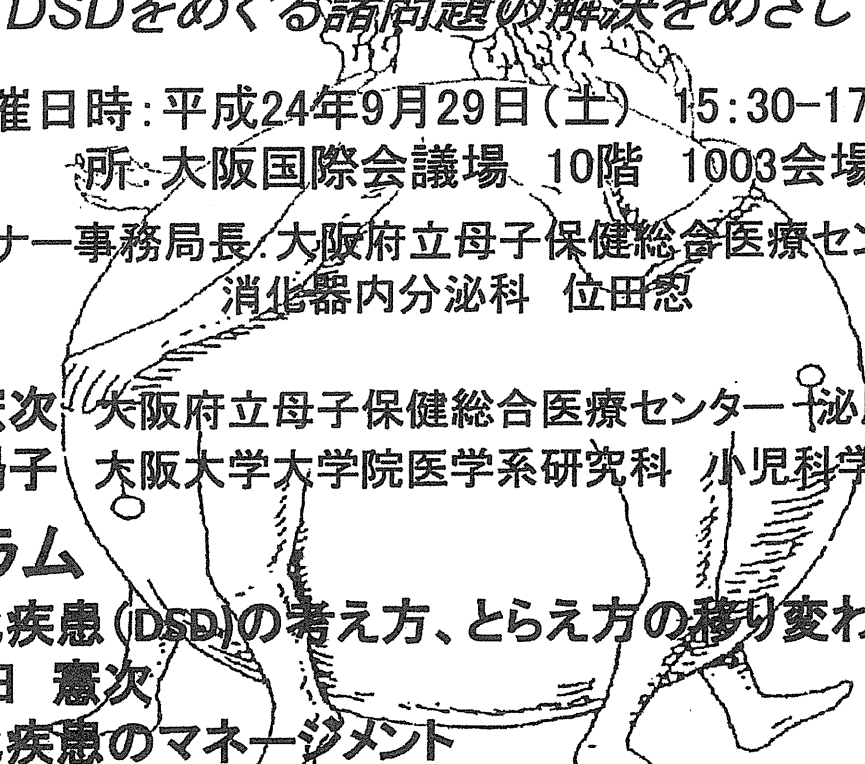

## 司　会

島田　憲次　大阪府立母子保健総合医療センター　泌尿器科
三善　陽子　大阪大学大学院医学系研究科　小児科学

## プログラム

1、性分化疾患（DSD）の考え方、とらえ方の移り変わり
　　島田　憲次
2、性分化疾患のマネージメント
　　堀川　玲子　国立成育医療研究センター　内分泌代謝科
3、性分化疾患の子どもと親への看護支援
　　石見　和世　大阪府立母子保健総合医療センター看護部
4、性分化疾患の子どもと親への思春期からの
　　セクシュアリティー支援
　　佐保　美奈子　大阪府立大学　地域保健学域　看護学類
5、フリーディスカッション

# 第2回 DSDセミナー in 大阪

## DSD:Disorder of sex development(性分化疾患)

## 多職種の関わりを基盤にした支援を目指して

医師・看護師・助産師・保健師・遺伝カウンセラー・臨床心理士など
多職種の皆様のご参加をお待ちしています。

日時：平成25年(2013年)12月14日(土) 11:00ー16:30(受付開始10:30)
場所：千里ライフサイエンスセンター 8階 801・802号室(地図裏面)
参加費：1000円(資料・昼食代を含む)

プログラム

**第1部 講演** 11:00 - 13:00

座長 大阪府立母子保健総合医療センター 泌尿器科 島田憲次
大阪大学大学院医学系研究科小児科学 大薗恵一

| | |
|---|---|
| 1. 性分化疾患初期対応の手引き解説 | 大阪府立母子保健総合医療センター 消化器・内分泌科 位田 忍 |
| 2. 性の健康と権利 | 大阪府立大学 人間社会学域 東 優子 |
| 3. 性自認 | こども心身研究所(野瀬クリニック) 仲野 由季子 |
| 4 DSDの診断と治療の実際 | 自治医科大学とちぎ医療センター 泌尿器科 中井 秀郎 |

**第2部 ケースカンファレンス** 13:20 - 14:50

座長 大阪大学大学院医学系研究科小児科学 三善陽子
大阪府立母子保健総合医療センター 看護部 石見和世

1. 滋賀医科大附属病院
2. 佐賀大学医学部附属病院・長崎大学病院
3. 大阪府立母子保健総合医療センター

**第3部 ワールド・カフェ** 15:00 - 16:00

進行 大阪府立大学 地域保健学域 佐保美奈子

**参加申し込み:11月30日までに下記までメールでお申し込みください。(先着90名)**
**dsd@mch.pref.osaka.jp**

主 催：DSDセミナー in 大阪 実行委員会(代表 島田憲次、位田忍、大薗恵一)
事務局：大阪府立母子保健総合医療センター 看護部 石見和世 0725-56-1220(代)

Clinical Endocrinology (2013) doi: 10.1111/cen.12379

ORIGINAL ARTICLE

# IMAGe syndrome: clinical and genetic implications based on investigations in three Japanese patients

Fumiko Kato*, Takashi Hamajima†, Tomonobu Hasegawa‡, Naoko Amano‡, Reiko Horikawa§, Gen Nishimura¶, Shinichi Nakashima*, Tomoko Fuke**, Shinichirou Sano**, Maki Fukami** and Tsutomu Ogata*

*Department of Pediatrics, Hamamatsu University School of Medicine, Hamamatsu, †Division of Endocrinology and Metabolism, Aichi Children's Health and Medical Center, Obu, ‡Department of Pediatrics, Keio University School of Medicine, §Division of Endocrinology and Metabolism, National Center for Child Health and Development, Tokyo, ¶Department of Radiology, Tokyo Metropolitan Children's Medical Center, Fuchu, and **Department of Molecular Endocrinology, National Research Institute for Child Health and Development, Tokyo, Japan

## Summary

**Objective** Arboleda *et al.* have recently shown that IMAGe (intra-uterine growth restriction, metaphyseal dysplasia, adrenal hypoplasia congenita and genital abnormalities) syndrome is caused by gain-of-function mutations of maternally expressed gene *CDKN1C* on chromosome 11p15.5. However, there is no other report describing clinical findings in patients with molecularly studied IMAGe syndrome. Here, we report clinical and molecular findings in Japanese patients.

**Patients** We studied a 46,XX patient aged 8·5 years (case 1) and two 46,XY patients aged 16·5 and 15·0 years (cases 2 and 3).

**Results** Clinical studies revealed not only IMAGe syndrome-compatible phenotypes in cases 1–3, but also hitherto undescribed findings including relative macrocephaly and apparently normal pituitary-gonadal endocrine function in cases 1–3, familial glucocorticoid deficiency (FGD)-like adrenal phenotype and the history of oligohydramnios in case 2, and arachnodactyly in case 3. Sequence analysis of *CDKN1C*, pyrosequencing-based methylation analysis of KvDMR1 and high-density oligonucleotide array comparative genome hybridization analysis for chromosome 11p15.5 were performed, showing an identical *de novo* and maternally inherited *CDKN1C* gain-of-function mutation (p.Asp274Asn) in cases 1 and 2, respectively, and no demonstrable abnormality in case 3.

**Conclusions** The results of cases 1 and 2 with *CDKN1C* mutation would argue the following: [1] relative macrocephaly is consistent with maternal expression of *CDKN1C* in most tissues and biparental expression of *CDKN1C* in the foetal brain; [2] FGD-like phenotype can result from *CDKN1C* mutation; and [3] genital abnormalities may primarily be ascribed to placental dysfunction. Furthermore, lack of *CDKN1C* mutation in case 3 implies genetic heterogeneity in IMAGe syndrome.

(Received 1 October 2013; returned for revision 24 November 2013; finally revised 26 November 2013; accepted 29 November 2013)

## Introduction

IMAGe syndrome is a multisystem developmental disorder named by the acronym of intra-uterine growth restriction (IUGR), metaphyseal dysplasia and adrenal hypoplasia congenita common to both 46,XY and 46,XX patients, and genital abnormalities specific to 46,XY patients.[1] In addition to these salient clinical features, hypercalciuria has been reported frequently in IMAGe syndrome.[1,2] This condition occurs not only as a sporadic form but also as a familial form.[1–3] Furthermore, transmission analysis in a large pedigree has revealed an absolute maternal inheritance of this condition, indicating the relevance of a maternally expressed gene to the development of IMAGe syndrome.[3]

Subsequently, Arboleda *et al.*[4] have mapped the causative gene to a ~17·2-Mb region on chromosome 11 by an identity-by-descent analysis in this large pedigree and performed targeted exon array capture and high-throughput genomic sequencing for this region in the affected family members and in other sporadic patients. Consequently, they have identified five different missense mutations in the maternally expressed gene *CDKN1C* (cyclin-dependent kinase inhibitor 1C) that resides on the imprinting control region 2 (ICR2) domain at chromosome 11p15.5 and encodes a negative regulator for cell proliferation.[4–6] Notably, all the missense mutations are clustered within a specific segment of PCNA-binding domain, and functional studies have implicated that these mutations have gain-of-function effects.[4] Thus, IMAGe syndrome appears to constitute a mirror image of Beckwith–Wiedemann syndrome (BWS) in terms of the

Correspondence: Dr. Tsutomu Ogata, Department of Pediatrics, Hamamatsu University School of Medicine, 1-20-1 Handayama, Higashi-ku, Hamamatsu 431-3192, Japan. Tel./Fax: +81 53 435 2310; E-mail: tomogata@hama-med.ac.jp

*CDKN1C* function, because multiple *CDKN1C* loss-of-function mutations have been identified in BWS with no mutation shared in common by IMAGe syndrome and BWS.[4,5]

However, several matters remain to be clarified in IMAGe syndrome, including phenotypic spectrum and underlying mechanism(s) for the development of each phenotype in *CDKN1C*-mutation-positive patients, and the presence or absence of genetic heterogeneity. Here, we report clinical and molecular findings in three patients with IMAGe syndrome and discuss these unresolved matters.

## Patients and methods

### Patients

We studied one previously described 46,XX patient (case 1)[7] and two hitherto unreported 46,XY patients (cases 2 and 3). In cases 1–3, no pathologic mutations were identified in the coding exons and their splice cites of *NR5A1* (*SF1*) and *NR0B1* (*DAX1*) relevant to adrenal hypoplasia,[8] and *MC2R, MRAP, STAR* and *NNT* involved in familial glucocorticoid deficiency (FGD).[9]

### Ethical approval and samples

This study was approved by the Institutional Review Board Committee at Hamamatsu University School of Medicine. Molecular studies were performed using leucocyte genomic DNA samples of cases 1–3 and the parents of cases 1 and 2, after obtaining written informed consent.

### Sequence analysis of CDKN1C

The coding exons 1 and 2 and their flanking splice sites were amplified by polymerase chain reaction (PCR) (Fig. 1a), using primers shown in Table S1. Subsequently, the PCR products were subjected to direct sequencing from both directions on ABI 3130 autosequencer (Life Technologies, Carlsbad, CA, USA). In this regard, if a nucleotide variation were present within the primer-binding site(s), this may cause a false-negative finding because of amplification failure of a mutation-positive allele. Thus, PNCA-binding domain was examined with different primer sets. To confirm a heterozygous mutation, the corresponding PCR products were subcloned with TOPO TA Cloning Kit (Life Technologies), and normal and mutant alleles were sequenced separately.

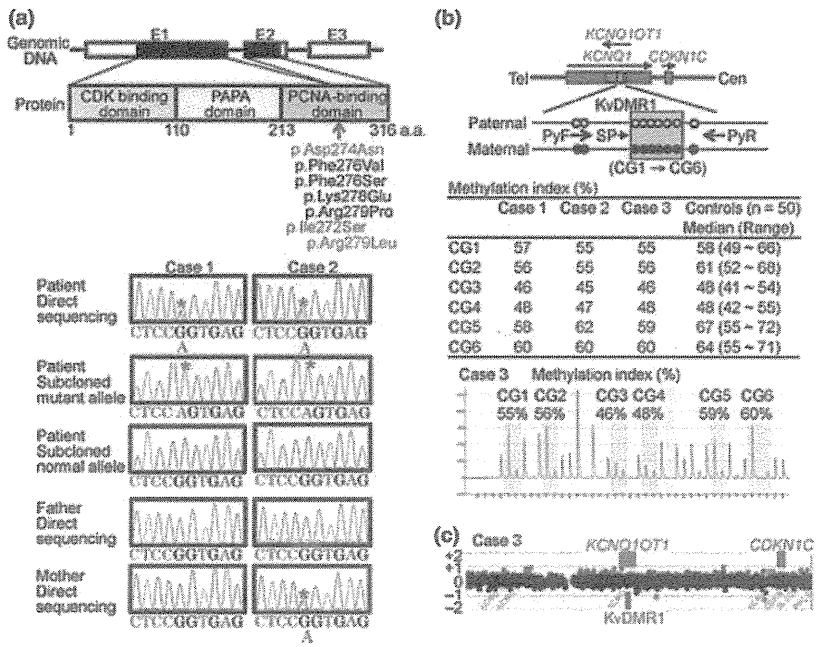


**Fig. 1** Summary of molecular studies. (a) Sequence analysis of *CDKN1C*. *CDKN1C* consists of three exons (E1–E3), and the black and white boxes denote the coding regions and the untranslated regions, respectively. CDKN1C protein is composed of 316 amino acids and contains CDK binding domain, PAPA domain and PCNA-binding domain. The p.Asp274Asn mutation found in this study and the previous study[4] is shown in red. The four mutations written in black have also been identified in IMAGe syndrome.[4] The pIle272Ser mutation written in green has been detected in atypical IMAGe syndrome lacking skeletal lesion,[22] and the pArg279Leu mutation written in blue has been found in SRS.[24] Electrochromatograms denote a *de novo* p.Asp274Asn mutation in case 1 and a maternally inherited p.Asp274Asn mutation in case 2. (b) Methylation analysis of KvDMR1 at the ICR2 domain. The cytosine residues at the CpG dinucleotides are unmethylated after paternal transmission (open circles) and methylated after maternal transmission (filled circles). *KCNQ1OT1* is a paternally expressed gene, and *KCNQ1* and *CDKN1C* are maternally expressed genes. The six CpG dinucleotides (CG1→CG6) examined by pyrosequencing are highlighted with a yellow rectangle, and the positions of PyF & PyR primers and SP are shown by thick arrows and a thin arrow, respectively. A pyrogram of case 3 is shown. (c) Array CGH analysis for chromosome 11p15.5 encompassing the ICR2 domain in case 3. A region encompassing KvDMR1 and *CDKN1C* is shown. Black, red and green dots denote signals indicative of the normal, the increased (>+0·5) and the decreased (<−1·0) copy numbers, respectively. Although several red and green signals are seen, there is no portion associated with ≥3 consecutive red or green signals.

### *Methylation analysis of KvDMR1 and array CGH analysis for chromosome 11p15.5*

Increased expression of *CDKN1C*, as well as gain-of-function mutations of *CDKN1C*, may lead to IMAGe syndrome. Such increased *CDKN1C* expression would occur in association with hypermethylated KvDMR1 (differentially methylated region 1) at the ICR2 domain, because *CDKN1C* is expressed when the *cis*-situated KvDMR1 is methylated as observed after maternal transmission and is repressed when the *cis*-situated KvDMR1 is unmethylated as observed after paternal transmission.[5] Thus, we performed pyrosequencing analysis for six CpG dinucleotides (CG1–CG6) within KvDMR1, using bisulphite-treated leucocyte genomic DNA samples (Fig. 1b). In brief, a 155-bp region was PCR-amplified with a primer set (PyF and PyR) for both methylated and unmethylated clones, and a sequence primer (SP) was hybridized to single-stranded PCR products (for PyF, PyR and SP sequences, see Table S1). Subsequently, methylation index (MI, the ratio of methylated clones) was obtained for each CpG dinucleotide, using PyroMark Q24 (Qiagen, Hilden, Germany). To define the reference ranges of MIs, 50 control subjects were similarly studied with permission.

Increased *CDKN1C* expression may also result from a copy number gain of the maternally inherited ICR2 domain. Thus, we performed high-density array CGH (comparative genomic hybridization) using a custom-build 33 088 oligonucleotide probes for chromosome 11p15.5 encompassing the ICR2 domain, together with ~10 000 reference probes for other chromosomal regions (Agilent Technologies, Santa Clara, CA, USA). The procedure was carried out as described in the manufacturer's instructions.

## Results

### *Clinical findings*

Detailed clinical findings are shown in Table 1. Cases 1–3 exhibited characteristic faces with frontal bossing, flat nasal root, low set ears and mild micrognathia, as well as short limbs. They had IUGR and postnatal growth failure. Notably, while birth and present length/height and weight were severely compromised, birth and present occipitofrontal circumference (OFC) were relatively well preserved. Radiological examinations revealed generalized osteopenia, delayed bone maturation and metaphyseal dysplasia with vertical sclerotic striations of the knee in cases 1–3, slender bones in cases 1 and 2, scoliosis in cases 2 and 3, arachnodactyly in case 3 and broad distal phalanx of the thumbs and great toes in case 2 (Fig. 2). Cases 1 and 3 experienced adrenal crisis in early infancy and received glucocorticoid and mineralocorticoid supplementation therapy since infancy. Case 2 had transient neonatal hyponatremia and several episodes of hypoglycaemia without electrolyte abnormality in childhood and was found to have hypoglycaemia and hyponatremia without hyperkalemia when he had severe viral gastroenteritis at 15·5 years of age. Thus, an adrenocorticotropic hormone stimulation test was performed after recovery from gastroenteritis, revealing poor cortisol response. Thereafter, he was placed on glucocorticoid supplementation therapy. As serum electrolytes were normal, mineralocorticoid supplementation therapy was not initiated. Genital abnormalities included cryptorchidism and small testes in cases 2 and 3, and hypospadias in case 3. However, pituitary-gonadal endocrine function was apparently normal in cases 1–3. Urine calcium secretion was borderline high or increased in cases 1–3, although serum calcium and calcium homeostasis-related factors were normal. In addition, feeding difficulties during infancy were observed in cases 1 and 2, but not in case 3, and oligohydramnios was noticed during the pregnancy of case 2. There was no body asymmetry in cases 1–3. Thus, clinical studies in cases 1–3 revealed not only IMAGe syndrome-compatible phenotypes, but also hitherto undescribed clinical finding (Table 2).

### *Sequence analysis of CDKN1C*

A heterozygous identical missense mutation (c.820G>A, p.Asp274Asn) was identified in cases 1 and 2 (Fig. 1a). This mutation occurred as a *de novo* event in case 1 and was inherited from the phenotypically normal mother in case 2. No demonstrable mutation was identified in case 3.

### *Methylation analysis of KvDMR1 and array CGH analysis for chromosome 11p15.5*

The MIs for CG1–CG6 were invariably within the normal range in cases 1–3 (Fig. 1b), and no discernible copy number alteration was identified in cases 1–3 (Fig. 1c). The results excluded maternal uniparental disomy involving KvDMR1, hypermethylation (epimutation) of the paternally inherited KvDMR1 and submicroscopic duplication involving the maternally derived ICR2 domain, as well as submicroscopic deletion affecting the paternally derived ICR2 domain.

## Discussion

### *CDKN1C mutations in IMAGe syndrome*

We identified a heterozygous *CDKN1C* missense mutation (Asp274Asn) in cases 1 and 2. This mutation has previously been detected in a patient with IMAGe syndrome.[4] Furthermore, *de novo* occurrence of the mutation in case 1 argues for the mutation being pathologic, and maternal transmission of the mutation in case 2 is consistent with *CDKN1C* being a maternally expressed gene. Thus, our results provide further evidence for specific missense mutations of *CDKN1C* being responsible for the development of IMAGe syndrome.

### *Clinical features in* CDKN1C*-mutation-positive cases 1 and 2*

Several matters are noteworthy with regard to clinical findings in *CDKN1C*-mutation-positive cases 1 and 2. First, although

**Table 1.** Clinical findings of cases 1–3

| | Case 1* | Case 2 | Case 3 |
|---|---|---|---|
| Karyotype | 46,XX | 46,XY | 46,XY |
| Present age (year) | 8·5 | 16·5 | 15·0 |
| Characteristic face | Yes | Yes | Yes |
| Pre- and postnatal growth | | | |
| Gestational age (week) | 35 | 37 | 38 |
| Birth length (cm) (SDS) | 37·0 (−3·5) | 40·0 (−4·0) | 41·0 (−4·3) |
| Birth weight (kg) (SDS) | 1·34 (−2·9) | 2·03 (−3·5) | 1·71 (−3·4) |
| Birth OFC (cm) (SDS) | 30·7 (−0·3) | 32·0 (−0·9) | 33·0 (−0·1) |
| Birth BMI (kg/m$^2$) (percentile) | 9·8 (<3) | 12·7 (50) | 10·1 (<3) |
| BMI (kg/m$^2$) at 2 years of age (SDS) | 14·2 (−1·8) | 13·0 (−3·4) | Unknown |
| Present height (cm) (SDS) | 92·8 (−6·2) | 124·7 (−7·8) | 135·2 (−5·1) |
| Present weight (kg) (SDS) | 16·0 (−1·9) | 25·4 (−3·5) | 30·4 (−2·6) |
| Present OFC (cm) (SDS) | 52·0 (−0·2) | 53·0 (−2·5) | Unknown |
| Present BMI (kg/m$^2$) (SDS) | 18·6 (+1·6) | 16·3 (−2·6) | 16·6 (−1·7) |
| Skeletal abnormality | | | |
| Examined age (year) | 5·5 | 16·5 | 15·0 |
| Generalized osteopenia | Yes | Yes | Yes |
| Delayed maturation | Yes | Yes | Yes |
| Metaphyseal dysplasia | Yes | Yes | Yes |
| Slender bones | Yes | Yes | No |
| Scoliosis | No | Yes | Yes |
| Arachnodactyly | No | No | Yes |
| Broad thumbs & big toes | No | Yes | No |
| Adrenal dysfunction | | | |
| Examined age (year) before therapy | 0·1 (39 days) | 15·5 | 0·5 (6 months) |
| MRI/CT | Undetectable | Undetectable | Undetectable |
| ACTH (pg/ml) | 9010 [19·9 ± 8·8] | 427 [22·9 ± 6·2] | >1000 [22·9 ± 6·2] |
| Cortisol (μg/dl) | 8·4 [8·3 ± 3·4] | 6·9 [9·5 ± 2·9] | <1·0 [9·5 ± 2·9] |
| After ACTH stimulation† | N.E. | 9·4 [> 20] | <1·0 [> 20] |
| Plasma renin activity (ng/ml/h) | N.E. | 6·0 [1·0 ± 0·1] | >25 [1·01 ± 0·14] |
| Active renin concentration (pg/ml) | 21 400 [2·5–21·4] | N.E. | N.E. |
| Aldosterone (ng/dl) | 6·9 [9·7 ± 4·5] | 5·2 [8·5 ± 1·4] | 4·1 [7·4 ± 2·2] |
| Na (mEq/l) | 122 [135–145] | 141 (127‡) [135–145] | 126 [135–145] |
| K (mEq/l) | 8·0 [3·7–4·8] | 4·2 (4·0‡) [3·7–4·8] | 6·5 [3·7–4·8] |
| Cl (mEq/l) | 86 [98–108] | 103 (98‡) [98–108] | 89 [98–108] |
| Glucocorticoid therapy | Yes (since 2 months) | Yes (since 15·5 years) | Yes (since 6 months) |
| Mineralocorticoid therapy | Yes (since 2 months) | No | Yes (since 6 months) |
| Genital abnormality | | | |
| Examined age (year) | 8·5 | 16·5 | 15·0 |
| Hypospadias | – | No | Yes (operated at 2 years) |
| Cryptorchidism | – | Yes (B) (operated at 2 years) | Yes (operated at 2 years) |
| Micropenis | – | No | No |
| Testis size (R & L) (ml) | – | 5 & 8 [13–20] | 4 & 10 [11–20] |
| Pubic hair (Tanner stage) | 1 [10·0 ± 1·4 years]§ | 4 [14·9 ± 0·9 years]¶ | 4 [14·9 ± 0·9 years]¶ |
| LH (mIU/ml) | <0·1 [<0·1–1·3] | 3·9 [0·2–7·8] | 4·8 [0·2–7·8] |
| After GnRH-stimulation** | 3·5 [1·6–4·8] | N.E. | N.E. |
| FSH (mIU/ml) | 0·7 [<0·1–5·4] | 4·2 [0·3–18·4] | 17·6 [0·3–18·4] |
| After GnRH-stimulation** | 12·0 [10·7–38·1] | N.E. | N.E. |
| Testosterone (ng/ml) | – | 4·3 [1·7–8·7] | 3·7 [1·7–8·7] |
| Calcium metabolism | | | |
| Examined age (year) | 8·5 | 16·5 | 15·0 |
| Calcium (mg/dl) | 9·7 [8·8–10·5] | 9·2 [8·9–10·6] | 9·8 [8·9–10·6] |
| Inorganic phosphate (mg/dl) | 3·9 [3·7–5·6] | 4·6 [3·1–5·0] | 3·8 [3·2–5·1] |
| Alkaline phosphatase (IU/l) | 458 [343–917] | 623 [225–680] | 309 [225–680] |
| Intact PTH (pg/ml) | 23 [10–65] | 43 [10–65] | 28 [10–65] |
| PTHrP (pmol/l) | N.E. | <1·1 [<1·1] | N.E. |

(continued)


*Clinical Endocrinology* (2013), **0**, 1–8

**Table 1.** (continued)

| | Case 1* | Case 2 | Case 3 |
|---|---|---|---|
| $1,25(OH)_2$ vitamin D (pg/ml) | 50 [13–79] | 67 [13–79] | 50 [13–79] |
| Urine calcium/creatinine ratio (mg/mg) | 0·82 [<0·25] | 0·24 [<0·25] | 0·44 [<0·25] |
| %TRP | 92 [80–96] | 95 [80–96] | 94 [80–96] |
| Others | Feeding difficulties | Feeding difficulties Oligohydramnios | |

SDS, standard deviation score; OFC, occipitofrontal circumference; BMI, body mass index; MRI, magnetic resonance imaging; CT, computed tomography; ACTH, adrenocorticotropic hormone; R, right; L, left; LH, luteinizing hormone; FSH, follicle-stimulating hormone; GnRH, gonadotropin-releasing hormone; PTH, parathyroid hormone; PTHrP, PTH-related protein; TRP, tubular reabsorption of phosphate; N.E., not examined; and B, bilateral.
Biochemical values indicate basal blood values, except for those specifically defined.
Birth and present length/height, weight, OFC and BMI have been assessed by sex- and gestational- or age-matched Japanese reference data reported in the literature[26,27] and in the Ministry of Health, Labor, and Welfare Database (http://www.e-stat.go.jp/SG1/estat/GL02020101.do).
The values in brackets represent age- and sex-matched reference values in Japanese children.[28]
The conversion factor to the SI unit: 0·220 for ACTH (pmol/l), 27·6 for cortisol (nmol/l), 0·028 for aldosterone (nmol/l), 3·46 for testosterone (nmol/l), 0·25 for calcium (nmol/l), 0·323 for inorganic phosphate (nmol/l), 0·106 for intact PTH (pmol/l), 2·40 for $1,25(OH)_2$ vitamin D (pmol/l) and 1·0 for plasma renin activity (μg/l/h), active renin concentration (ng/l), Na (nmol/l), K (nmol/l), Cl (nmol/l), LH (IU/l), FSH (IU/l), alkaline phosphatase (IU/l) and PTHrP (pmol/l).
*Clinical findings before 3 years of age have been reported previously.[7]
†ACTH 0·25 mg bolus i.v.; blood sampling at 60 min.
‡Electrolyte values at the time of severe gastroenteritis; other biochemical data in reference to adrenal dysfunction were obtained after recovery from gastroenteritis and before glucocorticoid supplementation therapy.
§Reference age for Tanner stage 2 breast development in Japanese girls.[29]
¶Reference age for Tanner stage 4 pubic hair development in Japanese boys.[29]
**GnRH 100 μg/m$^2$ bolus i.v.; blood sampling at 0, 30, 60, 90, and 120 min.

**Table 2.** Summary of clinical features of cases 1–3

| | Case 1 | Case 2 | Case 3 |
|---|---|---|---|
| *CDKN1C* mutation | Yes | Yes | No |
| Previously reported IMAGe syndrome-compatible phenotype | | | |
| IUGR | Yes | Yes | Yes |
| Metaphyseal dysplasia | Yes | Yes | Yes |
| Adrenal hypoplasia | Yes* | Yes* | Yes* |
| Genital abnormality | (Female) | Yes | Yes |
| Hypercalciura† | Yes | No | Yes |
| Hitherto undescribed findings | | | |
| Body habitus | Relative macrocephaly | Relative macrocephaly | Relative macrocephaly |
| Skeletal | | | Arachnodactyly Lack of slender bones |
| Adrenal | | FGD-like phenotype with no obvious mineralocorticoid deficiency | |
| Genital | Apparently normal pituitary-gonadal endocrine function | Apparently normal pituitary-gonadal endocrine function | Apparently normal pituitary-gonadal endocrine function |
| Others | Feeding difficulties | Feeding difficulties Oligohydramnios | |

IUGR, intrauterine growth retardation; and FGD, familial glucocorticoid deficiency.
*Undetectable on magnetic resonance imaging and/or computed tomography.
†Frequent but not invariable feature.

pre- and postnatal body growth was severely impaired, pre- and postnatal OFC was relatively well preserved. In this regard, while *CDKN1C* is preferentially expressed from the maternal allele in most tissues, it is biparentally expressed at least in the foetal brain.[10] This expression pattern would be relevant to the relative macrocephaly in IMAGe syndrome. Notably, the combination of severely compromised body growth and well-preserved OFC is also characteristic of Silver–Russell syndrome (SRS) resulting

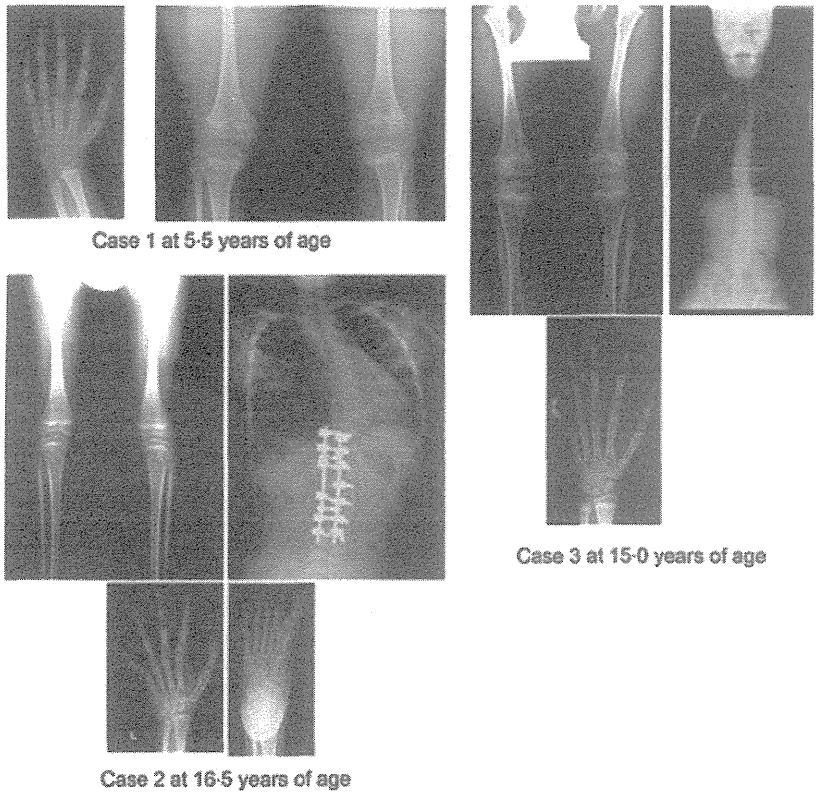


**Fig. 2** Representative skeletal roentgenograms in cases 1–3.

from *H19*-DMR hypomethylation (epimutation),[11] and this is primarily consistent with paternal expression of the growth-promoting gene *IGF2* in the body and biparental expression of *IGF2* in the brain.[12] Thus, loss-of-imprinting in the brain tissue appears to underlie relative macrocephaly in both IMAGe syndrome and SRS.

Second, skeletal abnormalities including metaphyseal dysplasia were identified in cases 1 and 2. In this regard, skeletal phenotype of mice lacking *Cdkn1c* is grossly opposite of parathyroid hormone-related protein (PTHrP)-null phenotype,[13,14] and PTHrP permits skeletal development at least in part by suppressing *Cdkn1c* expression.[15] Thus, while serum calcium and calcium homeostasis-related factors were normal in cases 1 and 2, dysregulated PTHrP and/or PTH/PTHrP receptor signalling might be relevant to skeletal abnormalities in patients with gain-of-function mutations of *CDKN1C*. In addition, such a possible signalling defect might also be relevant to the frequent occurrence of hypercalciuria in IMAGe syndrome.

Third, adrenal dysfunction was mild in case 2, while case 1 experienced adrenal crisis in infancy as previously reported in patients with *CDKN1C* mutations.[1,3,4] Indeed, adrenal phenotype of case 2 is similar to that of patients with FGD rather than adrenal hypoplasia.[8,9] Our results therefore would expand the clinical spectrum of adrenal dysfunction in patients with *CDKN1C* mutations. For adrenal dysfunction, cortisol and aldosterone values remained within the normal range at the time of adrenal crisis in case 1 (Table 1). However, as adrenocorticotropic hormone and active renin concentrations were markedly increased, the overall results would be consistent with primary hypoadrenalism, as has been described previously.[16] This notion would also apply to the adrenal dysfunction in case 3 who had apparently normal aldosterone value and markedly increased plasma renin activity at the time of adrenal crisis.

Lastly, although male case 2 had bilateral cryptorchidism and small testes, pituitary-gonadal endocrine function was apparently normal as was secondary sexual development. Previously reported patients with *CDKN1C* mutations, as well as those who have not been examined for *CDKN1C* mutations, also have undermasculinized external genitalia in the presence of apparently normal endocrine function and pubertal development.[1–4,17,18] Notably, an episode of oligohydramnios was found in case 2 and has also been described in a 46,XY IMAGe syndrome patient with cryptorchidism.[19] This may imply the presence of placental hypoplasia and resultant chorionic gonadotropin deficiency as an underlying factor for genital anomalies.[11] In support of this notion, imprinted genes are known to play a pivotal role in body and placental growth,[20] and SRS is often associated with oligohydramnios, placental hypoplasia and undermasculinization.[11,21]

### *Genetic heterogeneity in IMAGe syndrome*

Molecular data in case 3 imply the presence of genetic heterogeneity in IMAGe syndrome. Indeed, there was neither demonstrable *CDKN1C* mutation nor evidence for increased *CDKN1C* expression, while a pathologic mutation leading to gain-of-function or

increased expression of *CDKN1C* might reside on an unexamined region(s) such as promoter or enhancer sequences. In this regard, while case 3 showed IMAGe syndrome-compatible clinical features such as IUGR, metaphyseal dysplasia, adrenal hypoplasia and genital abnormalities, case 3 lacked slender bones and had arachnodactyly, in contrast to *CDKN1C*-mutation-positive cases 1 and 2. Such mild but discernible phenotypic variation might reflect the genetic heterogeneity. This matter might be clarified in the future by extensive studies such as exome or whole-genome sequencing. In particular, when such *CDKN1C*-mutation-negative patients with IMAGe syndrome-compatible phenotype have been accumulated, a novel gene(s) mutated in such patients may be identified. In this regard, if such a gene(s) exist, it is predicted to reside in the signal transduction pathway involving *CDKN1C*.

### *Relevance of CDKN1C mutations to atypical IMAGe syndrome and SRS*

*CDKN1C* mutations have also been identified in atypical IMAGe syndrome and SRS (Fig. 1a). Hamajima *et al.* revealed a maternally inherited p.Ile272Ser mutation in three siblings (two males and one female) who manifested IUGR and adrenal insufficiency, and male genital abnormalities, but had no skeletal lesion.[22] Similarly, Brioude *et al.* found a maternally transmitted p.Arg279Leu mutation in six relatives (all females) from a four-generation family who satisfied the SRS diagnostic criteria,[23,24] after studying 97 SRS patients without known causes of SRS, that is, hypomethylation (epimutation) of the *H19*-DMR, duplication of the ICR2 and maternal uniparental disomy for chromosome 7 (upd(7)mat).[24] Notably, although both mutations had no significant effect on a cell cycle, they were associated with increased protein stability that appears to be consistent with the gain-of-function effects.[22,24] Such increased stability was also found for IMAGe-associated missense mutant proteins,[22] and an altered cell cycle with a significantly higher proportion of cells in the G1 phase was shown for an IMAGe-associated p.Arg279Pro mutation.[24] It is possible therefore that relatively severe *CDKN1C* gain-of-function effects lead to IMAGe syndrome and relatively mild *CDKN1C* gain-of-function effects result in SRS, with intermediate *CDKN1C* gain-of-function effects being associated with atypical IMAGe syndrome.[24]

Thus, it would not be surprising that cases 1–3 also met the SRS diagnostic criteria (Table 3).[23,24] Indeed, cases 1–3, as well as *CDKN1C*-mutation-positive SRS patients,[24] exhibited pre- and post-natal growth failure with relative macrocephaly and frequently manifested feeding difficulties and/or low body mass index (BMI) at two years of age. However, while relative macrocephaly is usually obvious at birth in SRS patients with *H19*-DMR epimutations and upd(7)mat,[21,23,25] it is more obvious at 2 years of age than at birth in *CDKN1C*-mutation-positive SRS patients.[24] Furthermore, *CDKN1C*-mutation-positive SRS patients are free from body asymmetry,[24] as are typical and atypical IMAGe syndrome patients described in this study and in the previous studies.[1–4,7,22] Thus, SRS caused by *CDKN1C* mutations may be characterized by clinically discernible macrocephaly at two years of age and lack of body asymmetry.

**Table 3.** Silver–Russell syndrome phenotypes in cases 1–3 and in affected relatives reported by Brioude *et al.*

| | Case 1 | Case 2 | Case 3 | Brioude *et al.** |
|---|---|---|---|---|
| Mandatory criteria | | | | |
| IUGR† | Yes | Yes | Yes | 4/4 |
| Scoring system criteria | | | | |
| Postnatal short stature (≤−2 SDS) | Yes | Yes | Yes | 4/4 |
| Relative macrocephaly‡ | Yes | Yes | Yes | 4/4§ |
| Prominent forehead during early childhood | Yes | Yes | Yes | 4/4 |
| Body asymmetry | No | No | No | 0/4 |
| Feeding difficulties during early childhood and/or low BMI (<−2·0 SDS) around 2 years of age | Yes | Yes | Unknown | 3/4 (1/4 & 2/4)¶ |

IUGR, Intrauterine growth retardation; SDS, standard deviation score; and BMI, body mass index.
The SRS diagnostic criteria proposed by Netchine *et al.*[23] and Brioude *et al.*[24] (low BMI around 2 years of age is included in Brioude *et al.*, but not in Netchine *et al.*): The diagnosis of SRS is made, when mandatory criteria plus at least three of the five scoring system criteria are observed. For detailed clinical features in cases 1–3, see Table 1.
*While six relatives were found to have *CDKN1C* mutation, detailed clinical features have been obtained in four mutation-positive relatives.[24]
†Birth length and/or birth weight ≤−2 SDS for gestational age.
‡SDS for birth length or birth weight minus SDS for birth occipitofrontal circumference ≤−1·5.
§Relative macrocephaly is more obvious at 2 years of age (4/4) than at birth (2/4).
¶One patient is positive for feeding difficulties, and other two patients are positive for low BMI.

## Conclusion

In summary, we studied three patients with IMAGe syndrome. The results provide implications for phenotypic spectrum, underlying factor(s) in the development of each phenotype and genetic heterogeneity in IMAGe syndrome, as well as a phenotypic overlap between IMAGe syndrome and SRS. Further studies will permit to elucidate such matters.

## Funding

This study was supported in part by Grants-in-Aid for Scientific Research (A) (25253023) and for Scientific Research on Innovative Areas (22132004-A01) from the Ministry of Education, Culture, Sports, Science and Technology, by Grant for Research on Intractable Diseases from the Ministry of Health, Labor and Welfare (H24-048), and by Grants from National Center for Child Health and Development (23A-1, 24-7 and 25-10).

## Declaration of interest

The authors have nothing to declare.

## References


1 Vilain, E., Le Merrer, M., Lecointre, C. *et al.* (1999) IMAGe, a new clinical association of intrauterine growth retardation, metaphyseal dysplasia, adrenal hypoplasia congenita, and genital anomalies. *Journal of Clinical Endocrinology and Metabolism*, **84**, 4335–4340.

2 Balasubramanian, M., Sprigg, A. & Johnson, D.S. (2010) IMAGe syndrome: case report with a previously unreported feature and review of published literature. *American Journal of Medical Genetics A*, **152A**, 3138–3142.

3 Bergadá, I., Del Rey, G., Lapunzina, P. *et al.* (2005) Familial occurrence of the IMAGe association: additional clinical variants and a proposed mode of inheritance. *Journal of Clinical Endocrinology and Metabolism*, **90**, 3186–3190.

4 Arboleda, V.A., Lee, H., Parnaik, R. *et al.* (2012) Mutations in the PCNA-binding domain of CDKN1C cause IMAGe syndrome. *Nature Genetics*, **44**, 788–792.

5 Demars, J. & Gicquel, C. (2012) Epigenetic and genetic disturbance of the imprinted 11p15 region in Beckwith-Wiedemann and Silver-Russell syndromes. *Clinical Genetics*, **81**, 350–361.

6 Lee, M.-H., Reynisdottir, I. & Massague, J. (1995) Cloning of p57(KIP2), a cyclin-dependent kinase inhibitor with unique domain structure and tissue distribution. *Genes and Development*, **9**, 639–649.

7 Amano, N., Naoaki, H., Ishii, T. *et al.* (2008) Radiological evolution in IMAGe association: a case report. *American Journal of Medical Genetics A*, **146A**, 2130–2133.

8 El-Khairi, R., Martinez-Aguayo, A., Ferraz-de-Souza, B. *et al.* (2011) Role of DAX-1 (NR0B1) and steroidogenic factor-1 (NR5A1) in human adrenal function. *Endocrine Development*, **20**, 38–46.

9 Meimaridou, E., Hughes, C.R., Kowalczyk, J. *et al.* (2013) Familial glucocorticoid deficiency: new genes and mechanisms. *Molecular and Cellular Endocrinology*, **371**, 195–200.

10 Matsuoka, S., Thompson, J.S., Edwards, M.C. *et al.* (1996) Imprinting of the gene encoding a human cyclin-dependent kinase inhibitor, p57KIP2, on chromosome 11p15. *Proceedings of the National Academy of Sciences of the USA*, **93**, 3026–3030.

11 Yamazawa, K., Kagami, M., Nagai, T. *et al.* (2008) Molecular and clinical findings and their correlations in Silver-Russell syndrome: implications for a positive role of IGF2 in growth determination and differential imprinting regulation of the IGF2-H19 domain in bodies and placentas. *Journal of Molecular Medicine*, **86**, 1171–1181.

12 Ulaner, G.A., Yang, Y., Hu, J.F. *et al.* (2003) CTCF binding at the insulin-like growth factor-II (IGF2)/H19 imprinting control region is insufficient to regulate IGF2/H19 expression in human tissues. *Endocrinology*, **144**, 4420–4426.

13 Zhang, P., Leigeois, N.J., Wong, C. *et al.* (1997) Altered cell differentiation and proliferation in mice lacking p57(KIP2) indicates a role in Beckwith-Wiedemann syndrome. *Nature*, **387**, 151–158.

14 Karaplis, A.C., Luz, A., Glowacki, J. *et al.* (1994) Lethal skeletal dysplasia from targeted disruption of the parathyroid hormone-related peptide gene. *Genes & Development*, **8**, 277–289.

15 MacLean, H.E., Guo, J., Knight, M.C. *et al.* (2004) The cyclin-dependent kinase inhibitor p57(Kip2) mediates proliferative actions of PTHrP in chondrocytes. *Journal of Clinical Investigation*, **113**, 1334–1343.

16 Stewart, P.M. & Krone, N.P. (2011) The adrenal cortex. In: S. Melmed, K.S. Polonsky, P.R. Larsen, H.N. Kronenberg eds. Williams Textbook of Endocrinology, 12th edn. Elsevier, Saunders, 479–577.

17 Lienhardt, A., Mas, J.C., Kalifa, G. *et al.* (2002) IMAGe association: additional clinical features and evidence for recessive autosomal inheritance. *Hormone Research*, **57**(Suppl 2), 71–78.

18 Pedreira, C.C., Savarirayan, R. & Zacharin, M.R. (2004) IMAGe syndrome: a complex disorder affecting growth, adrenal and gonadal function, and skeletal development. *Journal of Pediatrics*, **144**, 274–277.

19 Ko, J.M., Lee, J.H., Kim, G.H. *et al.* (2007) A case of a Korean newborn with IMAGe association presenting with hyperpigmented skin at birth. *European Journal of Pediatrics*, **166**, 879–880.

20 Fowden, A.L., Sibley, C., Reik, W. *et al.* (2006) Imprinted genes, placental development and fetal growth. *Hormone Research*, **65** (Suppl 3), 50–58.

21 Wakeling, E.L., Amero, S.A., Alders, M. *et al.* (2010) Epigenotype-phenotype correlations in Silver-Russell syndrome. *Journal of Medical Genetics*, **47**, 760–768.

22 Hamajima, N., Johmura, Y., Suzuki, S. *et al.* (2013) Increased protein stability of CDKN1C causes a gain-of-function phenotype in patients with IMAGe syndrome. *PLoS ONE*, **8**, e75137.

23 Netchine, I., Rossignol, S., Dufourg, M.N. *et al.* (2007) 11p15 imprinting center region 1 loss of methylation is a common and specific cause of typical Russell-Silver syndrome: clinical scoring system and epigenetic-phenotypic correlations. *Journal of Clinical Endocrinology and Metabolism*, **92**, 3148–3154.

24 Brioude, F., Oliver-Petit, I., Blaise, A. *et al.* (2013) CDKN1C mutation affecting the PCNA-binding domain as a cause of familial Russell Silver syndrome. *Journal of Medical Genetics*, **50**, 823–830.

25 Fuke, T., Mizuno, S., Nagai, T. *et al.* (2013) Molecular and clinical studies in 138 Japanese patients with Silver-Russell syndrome. *PLoS ONE*, **8**, e60105.

26 Suwa, S., Tachibana, K., Maesaka, H. *et al.* (1992) Longitudinal standards for height and height velocity for Japanese children from birth to maturity. *Clinical Pediatric Endocrinology*, **1**, 5–14.

27 Inokuchi, M., Matsuo, N., Anzo, M. *et al.* (2007) Body mass index reference values (mean and SD) for Japanese children. *Acta Paediatrica*, **96**, 1674–1676.

28 Japan Public Health Association. (1996) Normal Biochemical Values in Japanese Children. Sanko Press, Tokyo, (in Japanese).

29 Matsuo, N. (1993) Skeletal and sexual maturation in Japanese children. *Clinical Pediatric Endocrinology*, **2**(Suppl), 1–4.


## Supporting Information

Additional Supporting Information may be found in the online version of this article:

**Table S1.** Primers utilized in this study.

*Endocrine Journal* 2013, **60** (12), 1329-1334

ORIGINAL

# Critical role of Yp inversion in *PRKX/PRKY*-mediated Xp;Yp translocation in a patient with 45,X testicular disorder of sex development

Shinichi Nakashima[1)], Yoriko Watanabe[2)], Junichiro Okada[2)], Hiroyuki Ono[1)], Eiko Nagata[1)], Maki Fukami[3)] and Tsutomu Ogata[1)]

[1)]*Department of Pediatrics, Hamamatsu University School of Medicine, Hamamatsu 431-3192, Japan*
[2)]*Department of Pediatrics, Kurume University School of Medicine, Kurume 830-0011, Japan*
[3)]*Department of Molecular Endocrinology, National Research Institute for Child Health and Development, Tokyo 157-8535, Japan*

**Abstract.** 45,X testicular disorder of sex development (TDSD), previously known as 45,X maleness, with unbalanced Xp;Yp translocation is an extremely rare condition caused by concomitant occurrence of loss of an X chromosome of maternal origin and an aberrant Xp;Yp translocation during paternal meiosis. We identified a Japanese male infant with an apparently 45,X karyotype who exhibited chondrodysplasia punctata and growth failure. Cytogenetic analysis revealed a 45,X.ish der(X)t(X;Y)(p22.33;p11.2)(DXZ1+,SRY+) karyotype. Array comparative genome hybridization analysis showed a simple Xp terminal deletion involving *SHOX* and *ARSE* with the breakpoint just centromeric to *PRKX*, and an apparently complex Yp translocation with the middle Yp breakpoint just telomeric to *PRKY* and the centromeric and the telomeric Yp breakpoints around the long inverted repeats for the generation of a common paracentric Yp inversion. Subsequently, a long PCR product was obtained with an X-specific and a Y-specific primers that were designed on the assumption of the presence of a Yp inversion that permits the alignment of *PRKX* and *PRKY* in the same direction, and the translocation fusion point was determined to reside within a 246 bp X-Y homologous segment at the "hot spot A" in the 5' region of *PRKX/PRKY*, by sequential direct sequencing for the long PCR product. These results argue not only for the presence of rare 45,X-TDSD with Xp;Yp translocation, but also for a critical role of a common paracentric Yp inversion in the occurrence of *PRKX/PRKY*-mediated unbalanced Xp;Yp translocation.

*Key words*: 45,X testicular DSD, Xp;Yp translocation, *PRKX/PRKY*, Yp inversion

**45,X TESTICULAR DISORDER** of sex development (TDSD) (previously known as 45,X maleness) with unbalanced Xp;Yp translocation is an extremely rare condition caused by concomitant occurrence of loss of an X chromosome of maternal origin and an aberrant Xp;Yp translocation during paternal meiosis [1, 2]. To our knowledge, this condition has been documented only in two patients [1, 2], although another 45,X-TDSD patient with apparent mosaicism for normal X chromosome and abnormal der(X)t(Xp;Yp) chromosome harboring *SRY* has also been documented [3].

For the unbalanced Xp;Yp translocation, previous studies in patients with *SRY*-positive 45,X-TDSD and 46,XX-TDSD (previously known as 46,XX maleness) and in those with *SRY*-negative 46,XY gonadal dysgenesis (previously known as 46,XY femaleness) have indicated the frequent occurrence of aberrant translocations between the homologous genes *PRKX* and *PRKY* [4-7]. In particular, most *PRKX/PRKY*-mediated translocations have taken place at two hot spots, *i.e.*, the "hot spot A" at the 5' sequence that shares 97% sequence similarity over 1.7 kb and even 98.7% sequence similarity over 1.2 kb and the "hot spot B" around the C-terminal coding region that shares 90% sequence similarity over 2 kb and even 96% sequence similarity over 1 kb [5]. In this regard, although such translocations are predicted to occur when *PRKX* and *PRKY* are aligned in the same direction, *PRKX* and *PRKY* are usually oriented in a reverse direction. However, *PRKX* and *PRKY* are aligned in the same direction in a subgroup of males with a common ~3.5 Mb paracentric Yp

Submitted Aug. 11, 2013; Accepted Sep. 6, 2013 as EJ13-0334
Released online in J-STAGE as advance publication Oct. 3, 2013
Correspondence to: Tsutomu Ogata, Department of Pediatrics, Hamamatsu University School of Medicine, 1-20-1 Handayama, Higashi-ku, Hamamatsu 431-3192, Japan.
E-mail: tomogata@hama-med.ac.jp

inversion probably caused by a homologous recombination between ~300 kb long inverted repeats [7, 8]. It has been suggested, therefore, that *PRKX/PRKY*-mediated translocations are prone to occur in Yp inversion positive males [7, 9].

Here, we report a 45,X-TDSD patient with Xp;Yp translocation. Cytogenetic and molecular studies in this patient argue not only for the presence of rare 45,X-TDSD with Xp;Yp translocation, but also for a critical role of a common paracentric Yp inversion in the occurrence of *PRKX/PRKY*-mediated unbalanced Xp;Yp translocation.

## Case Report

### *Patient*

This Japanese patient was referred to Kurume University Hospital at 28 weeks of gestation because of intrauterine growth retardation and mild short limbs that were identified by routine fetal ultrasound examinations. Subsequent pregnant course was uneventful, although he remained small for gestational age. The non-consanguineous parents were clinically normal.

He was born at 38 weeks of gestation after an uncomplicated vaginal delivery. His birth length was 40.2 cm (–3.4 SD), birth weight 2.29 kg (–2.2 SD), and birth occipitofrontal circumference (OFC) 28.8 cm (–3.0 SD). Physical examination revealed relatively short limbs and depressed nasal bridge. External genitalia were well masculinized. There were no discernible Turner syndrome soft tissue and visceral features, such as webbed neck, lymphedema, and cardiovascular and renal lesions. Radiological studies showed atlantoaxial subluxation and stippled calcifications at the bilateral proximal humeri, proximal femur, proximal tibias, and ankles, and neonatal audiometry tests revealed hearing loss (right 50 dB, left 80 dB). Thus, he was diagnosed as having X-linked recessive chondrodysplasia punctata (CDPX1). On the last examination at six months of age, he manifested severe growth failure, with a length of 55.7 cm (–5.0 SD), a weight of 5.20 kg (–3.1 SD), and an OFC of 41.0 cm (–1.8 SD).

### *Cytogenetic studies*

G-banding analysis was performed at a 550-band resolution level, indicating a 45,add(X)(p22.33) karyotype in all the 50 lymphocytes examined. Fluorescence *in situ* hybridization analysis delineated positive signals for *DXZ1* and *SRY* on the same chromosome in all the 200 metaphases examined. Thus, his karyotype was determined as 45,X.ish der(X)t(X;Y)(p22.33;p11.2)(DXZ1+,SRY+). Parental karyotypes were apparently normal.

### *Array comparative genome hybridization analysis (CGH)*

Oligonucleotide-based array CGH was performed for leukocyte genomic DNA, using (1) the Agilent G4447A Sure Print G3 Human CGH 1X1M Oligo Microarray kit containing 1 million catalog probes for the whole genome (Agilent Technologies, Santa Clara, CA, USA); and (2) a custom-build array containing 857,877 probes for the X-differential region and 54,388 probes for the Y-differential region, as well as ~10,000 reference probes for other chromosomal region. The procedure was as described in the manufacturer's instructions.

Array CGH showed a ~3,670,000 bp simple Xp terminal deletion involving *SHOX* and *ARSE*, with the breakpoint around the *PRKX* "hot spot A", and an apparently complex Yp translocation involving a ~6,120,000 bp terminal Yp region and a ~2,590,000 bp region between ~7,100,000 bp and ~9,690,000 bp from the Yp telomere, with the middle Yp breakpoint around the *PRKY* "hot spot A" (Fig. 1). Furthermore, the centromeric and the telomeric Yp breakpoints resided around the long inverted repeats for the common ~3.5 Mb paracentric Yp inversion [8]. These findings indicated that the paternal Y chromosome was accompanied by a paracentric Yp inversion, and that the *SRY*-positive X chromosome was generated by a simple Xp;Yp translocation at the *PRKX/PRKY* "hot spot A".

### *Determination of the translocation fusion point*

To determine the translocation fusion point, we first performed PCR analysis using multiple primers for Xp-specific and Yp-specific loci around the breakpoints indicated by array CGH (Table 1). The Xp breakpoint was localized to a ~2,000 bp region between *XPBP3* and *XPBP4* (*XPBP1–XPBP4* were first designated in this study). While the results of Y-specific loci were apparently complex, they were interpreted as indicative of a single Yp breakpoint at a ~337,000 bp region between *PRKY* and *TBL1Y*, on the assumption of the presence of a paracentric Yp inversion (Fig. 2A).

Subsequently, long PCR was carried out using multiple primer sets for the localized Xp and Yp breakpoint segments, and a ~5.4 kb long PCR product was obtained with an Xp-specific primer and a Yp-specific primer (Table 2). Finally, direct sequencing was sequentially performed for the long PCR product, and the translocation fusion point

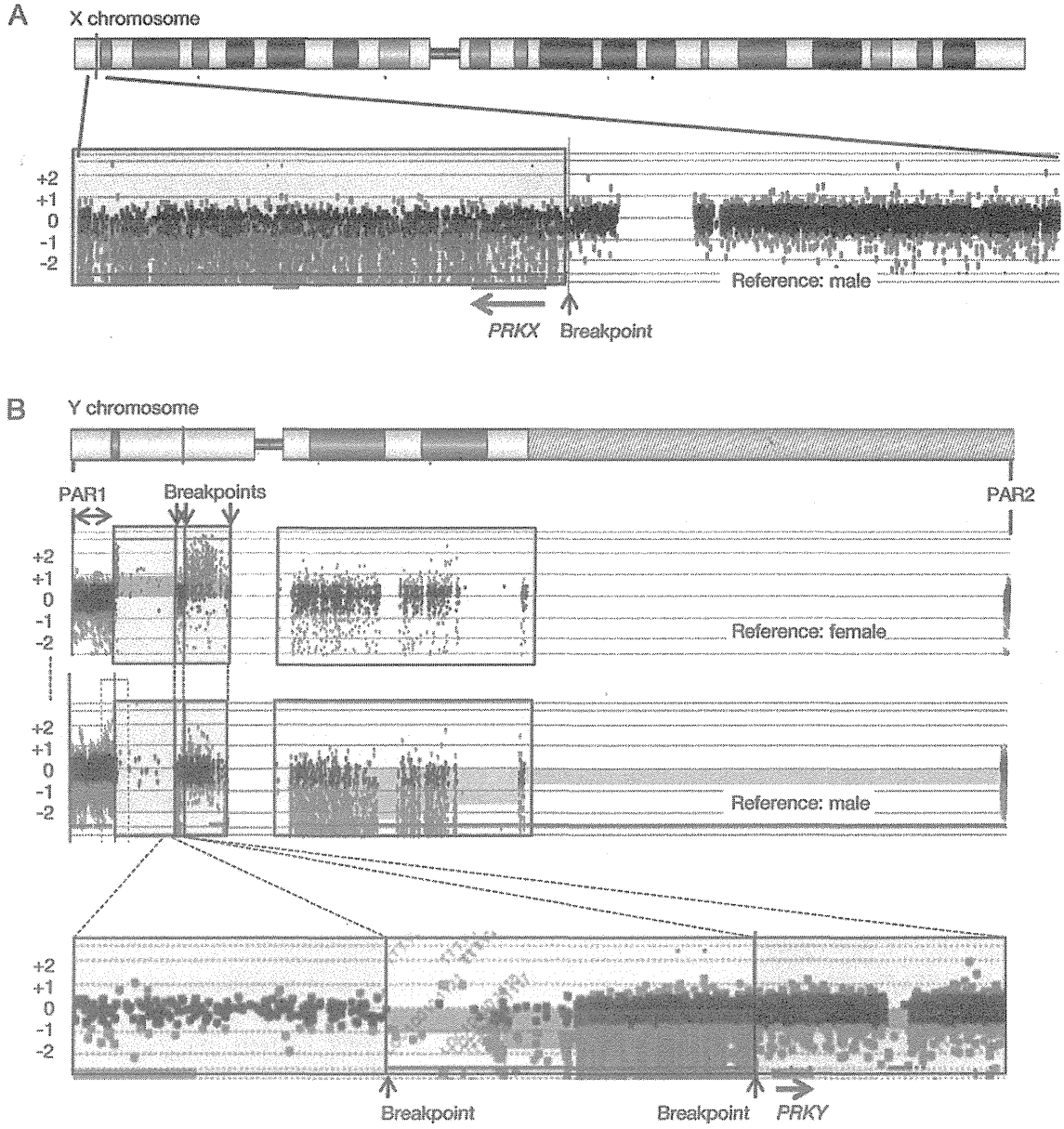


**Fig. 1** Representative results of array CGH analysis. The black, the red, and the green dots denote signals indicative of the normal, the increased (> +0.5), and the decreased (< –1.0) copy numbers, respectively.
(A) A simple Xp terminal deletion with the breakpoint just centromeric to *PRKX*. An X-differential region encompassing the breakpoint is magnified. The red arrow indicates the transcriptional direction of *PRKX*. The data have been obtained with a custom-build high density probes for the X-differential region, using a genomic DNA sample from a normal male as a reference. The deleted region is highlighted with light blue.
(B) An apparently complex Yp translocation with the middle breakpoints just telomeric to *PRKY*. The blue arrow indicates the transcriptional direction of *PRKY*. The upper and the middle array findings have been obtained with 1 million catalog probes for the whole genome, using genomic DNA samples from a normal male and a normal female as references, and the lower array finding have been obtained with a custom-build high density probes for the Y-differential region, using a genomic DNA sample from a normal male as a reference. The data indicate the presence of two Y-differential regions (highlighted with light orange) and the absence of the remaining Y-differential region including a small region between the two positive Y-differential regions (highlighted with light yellow), as well as the single copies of the short arm and long arm pseudoautosomal regions (PAR1 and PAR2).

**Table 1** Primers utilized in the localization of the translocation fusion point.

| Locus (STS) | Forward | Reverse | Amplified segment[a] | AT | Results |
|---|---|---|---|---|---|
| X-specific locus | | | | | |
| *XPBP1* | GCTGTCTCCCATTCCTGAGA | GCCCTCACCAGACACTGAAT | 3,663,463 ~ 3,663,700 bp | 58 | – |
| *XPBP2* | CCATGCACTCTTGCTGGTAA | CGTGCATTAAATGTGATCGTG | 3,665,692 ~ 3,665,904 bp | 58 | – |
| *XPBP3* | GGGTGGTTAGTGTGACCCAG | ACAATGAGCTGCCTCCCAAA | 3,671,443 ~ 3,671,599 bp | 58 | – |
| *XPBP4* | CCCTTCCCTCCCTTCCTTCT | GAATGGGCACGAAAATCATGCT | 3,673,439 ~ 3,673,639 bp | 58 | + |
| Y-specific locus | | | | | |
| *SHGC-79134* | TATCTTTGTTTCTTGCAGCGTG | TGGAAGTGGGAGTGGAGATAAA | 6,104,095 ~ 6,10,4376 bp | 60 | + |
| *G65838* (sY605) | ACCTCCGAAGACTGAACCAG | CCCTTGAGTCCACAGAGTCC | 6,616,473 ~ 6,61,6751 bp | 58 | – |
| *AMELY* (sY276) | CCTACCGCATCAGTGAATTTC | TCTGTATGTGGAGTACACATGG | 6,736,679 ~ 6,736,894 bp | 58 | – |
| *TBL1Y* (sY2228) | CTCTGTGTCACCCCCTGC | GGAGAAAAGGAAAAGAGCCAGTA | 6,910,077 ~ 6,910,300 bp | 58 | – |
| *PRKY* (sY1817) | GGAGCTAGAAGGAAAAGCATGA | GGCTGGAGGCTGATCATGAT | 7,246,851 ~ 7,247,177 bp | 60 | + |
| *G66267* (sY2183) | CCGTGGAGTGCTACACAGAC | TGCTTATGATTATGGCCTCCA | 8,668,480 ~ 8,668,754 bp | 60 | + |
| *TTTY20* (sY1249) | ACATGGGATCACAGGCTACC | TTTTTGAGGGACTTTCAGCTTC | 9,170,480 ~ 9,170,945 bp | 60 | + |
| *G75495* (sY1250) | TTTTTCTAACCTTGCCTGCG | TGCAGAGAAGCAGCCTACAA | 9,399,782 ~ 9,400,274 bp | 60 | + |
| *G75489* (sY1243) | ATCTGCACACTTGGGTAGGC | GAGGAAATGCAGAATTTGGG | 9,465,779 ~ 9,466,271 bp | 60 | + |
| *G75490* (sY1244) | GCTACTTGTGAATCACGCCA | TGCATATTTCGAAGCATTGTC | 9,756,903 ~ 9,757,402 bp | 58 | – |

*XPBP1–XPBP4* are named in this study and loci and the corresponding primers
[a], Physical length from the Xp/Yp telomere (according to GRCh37). AT: annealing temperature (°C)
The (+) and (–) symbols represent the presence and the absence of the examined loci, respectively.

was determined to reside within a 246 bp homologous segment at the *PRKX/PRKY* "hot spot A", by sequencing with the primers shown in Table 2 (Fig. 2B).

## Discussion

We identified a 45,X-TDSD patient with Xp;Yp translocation. To our knowledge, this is the third case with this condition. Consistent with such rarity, the frequency of 45,X-TDSD with Xp;Yp translocation has been estimated as ~1 of $6\times10^7$ livebirths, on the basis of the prevalence of loss of maternally derived X chromosome and that of aberrant Xp;Yp translocation during paternal meiosis [1].

The precise Xp;Yp translocation fusion point was determined to reside within a 246 bp segment at the "hot spot A". Although the precise structure of the paternal Y chromosome was not examined because of his refusal for genetic studies other than G-banding, the results argue for the occurrence of aberrant translocation between a normal X chromosome and a Y chromosome with a paracentric Yp inversion involving *PRKY* during paternal meiosis (Fig. 2A) [7, 9, 10]. Thus, the results would provide further support for the notion that a paracentric Yp inversion constitute an underlying factor for the generation of *PRKX/PRKX*-mediated Xp;Yp translocation [7]. In addition, the common ~3.5 Mb Yp inversion mediated by long inverted repeats appears to be present in a certain fraction of Japanese males as well as in ~one-third of European males [7, 8].

Precise Xp;Yp translocation fusion points have been determined at least in a single 45,X-TDSD patient and seven 46,XX-TDSD patients of European origin [4-6], although the presence of a paracentric Yp inversion has been shown in only one of the eight patients [6, 7]. Notably, the fusion points reside at the "hot spot A" in six of the eight patients and at the "hot spot B" in the remaining two patients [4-6]. Furthermore, the fusion point at the "hot spot A" appears to be identical in our patient and four of the six patients reported in the literature [5, 6]. Thus, the 246 bp homologous segment would be regarded as the "remarkable hot spot" for the unbalanced Xp;Yp translocations in males with a paracentric Yp inversion.

The genetic findings are primarily consistent with clinical phenotypes of this patient. Indeed, male sex development is compatible with the presence of *SRY* [11], CDPX1 phenotype (*e.g.*, stippled calcifications, depressed nasal bridge, and hearing loss) is ascribed to loss of *ARSE* [12], and growth failure and relatively short limbs are explainable by *SHOX* haploinsufficiency and chromosome imbalance as well as loss of *ARSE* [12-14]. Although this patient had no Turner-like soft tissue and visceral features, this would also be compatible with the structure of the der(X) chromosome. It has been suggested that such soft tissue and visceral features are deformational consequences

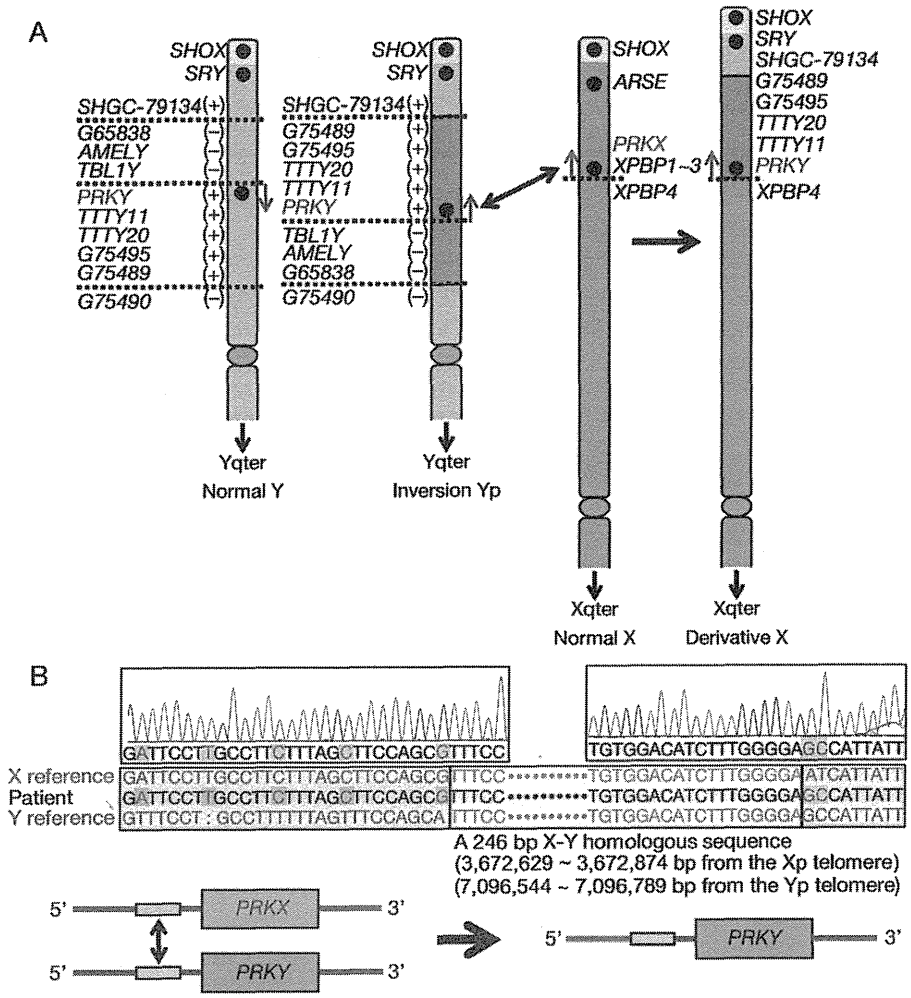


**Fig. 2** *PRKX-PRKY*-mediated translocation in the presence of a paracentric Yp inversion.
(A) Schematic representation of the aberrant translocation. The yellow, the pink, the blue, and the green segments denote the short arm pseudoautosomal region, the X-differential region, the Y-differential region, and the Y-differential inverted region, respectively. The (+) and (–) symbols indicate the presence and absence of the loci examined by standard PCR analysis. The data of the Y-specific loci is explained by a single breakpoint, on the assumption of a paracentric Yp inversion in the father. The red arrow indicates the transcriptional direction of *PRKX*, and the blue arrow denotes the transcriptional direction of *PRKY* that is aligned in the same orientation as *PRKX* in the presence of the Yp inversion.
(B) Determination of the translocation fusion point at the "hot spot A" in the 5' region of *PRKX/PRKY* of this patient. Direct sequencing of the long PCR product obtained with an X-specific and a Y-specific primer has shown the presence of X-specific five nucleotides (highlighted with red letters and yellow background) in the centromeric portion and the Y-specific two nucleotides (highlighted with blue letters and yellow background) in the telomeric portion. Thus, the translocation fusion point is located within an X-Y homologous 246 bp segment (indicated by a yellow rectangle) between the X-compatible sequence (indicated by a red rectangle) and the Y-compatible sequence (indicated by a blue rectangle), as illustrated in the below schema.

**Table 2** Primers utilized in the determination of the translocation fusion point

| | Primer sequence (5' → 3') | Primer position[a] | AT |
|---|---|---|---|
| Long PCR | | | |
| X-specific region | CAGTGGATTTAGCTCAGAGGCAGAGAAT | 3,673,743 ~ 3,673,770 bp | 66 |
| Y-specific region | GCTGGAGAGCTGAAAAGCAATGAGATAG | 7,100,894 ~ 7,100,921 bp | 66 |
| Direct sequencing of the long PCR product | | | |
| X-specific boundary | AGCCTGGGTGACAGAGAAAG | 3,672,963 ~ 3,672,982 bp | 58 |
| Y-specific boundary | ACTACCTGGGGCCACTTTCT | 7,096,924 ~ 7,096,943 bp | 58 |

[a] Physical length from the Xp/Yp telomere (according to GRCh37). AT: annealing temperature (°C)

explained as a malformation sequence initiated by lymphatic hypoplasia [15], and that lymphatic hypoplasia is caused by haploinsufficiency of a putative lymphogenic gene located between *DMD* and *MAOA* at the middle part of Xp and between *DYS255* and *PABY* at the distal part of Yp [16, 17]. Since the *DYS255–PABY* region resides distal to the inverted Yp portion, it is predicted that the putative Y-linked lymphogenic gene is translocated onto the der(X) chromosome, so that the putative lymphogenic gene is present in two copies in this patient, as in normal individuals.

In summary, the present results argue for the presence of rare 45,X-TDSD with Xp;Yp translocation, and for a critical role of a common paracentric Yp inversion in the occurrence of *PRKX/PRKY*-mediated Xp;Yp translocation.

## Acknowledgments

This work was Supported in part by Grants-in-Aid for Scientific Research on Innovative Areas (22132004-A01) from the Ministry of Education, Culture, Sports, Science and Technology, by Grant for Research on Intractable Diseases from the Ministry of Health, Labor and Welfare (H24-048), and by Grants from National Center for Child Health and Development (23A-1 and 24-7).

## Disclosure Summary

All authors have nothing to disclose.

## References

1. Weil D, Portnoï MF, Levilliers J, Wang I, Mathieu M, et al. (1993) A 45,X male with an X;Y translocation: implications for the mapping of the genes responsible for Turner syndrome and X-linked chondrodysplasia punctata. *Hum Mol Genet* 2: 1853–1856.
2. Stuppia L, Calabrese G, Borrelli P, Gatta V, Morizio E, et al. (1999) Loss of the SHOX gene associated with Leri-Weill dyschondrosteosis in a 45,X male. *J Med Genet* 36: 711–713.
3. Chernykh VB, Vyatkina SV, Antonenko VG, Shilova NV, Zolotukhina TV, et al. (2008) Unique mosaic X/Y translocation/insertion in infant 45,X male. *Am J Med Genet A* 146A: 3195–3197.
4. Weil D, Wang I, Dietrich A, Poustka A, Weissenbach J, et al. (1994) Highly homologous loci on the X and Y chromosomes are hot-spots for ectopic recombinations leading to XX maleness. *Nat Genet* 7: 414–419.
5. Wang I, Weil D, Levilliers J, Affara NA, de la Chapelle A, et al. (1995) Prevalence and molecular analysis of two hot spots for ectopic recombination leading to XX maleness. *Genomics* 28: 52–58.
6. Schiebel K, Winkelmann M, Mertz A, Xu X, Page DC, et al. (1997) Abnormal XY interchange between a novel isolated protein kinase gene, PRKY, and its homologue, PRKX, accounts for one third of all (Y+)XX males and (Y–)XY females. *Hum Mol Genet* 6: 1985–1989.
7. Jobling MA, Williams GA, Schiebel GA Pandya GA, McElreavey GA, et al. (1998) A selective difference between human Y-chromosomal DNA haplotypes. *Curr Biol* 8: 1391–1394.
8. Tilford CA, Kuroda-Kawaguchi T, Skaletsky H, Rozen S, Brown LG, et al. (2001) A physical map of the human Y chromosome. *Nature* 409: 943–945.
9. Sharp A, Kusz K, Jaruzelska J, Tapper W, Szarras-Czapnik M, et al. (2005) Variability of sexual phenotype in 46,XX(SRY+) patients: the influence of spreading X inactivation versus position effects. *J Med Genet* 42: 420–427.
10. McElreavey K, Cortes LS (2001) X-Y translocations and sex differentiation. *Semin Reprod Med* 19: 133–139.
11. Sinclair AH, Berta P, Palmer MS, Hawkins JR, Griffiths BL, et al. (1990) A gene from the human sex-determining region encodes a protein with homology to a conserved DNA-binding motif. *Nature* 346: 240–244.
12. Franco B, Meroni G, Parenti G, Levilliers J, Bernard L, et al. (1995) A cluster of sulfatase genes on Xp22.3: mutations in chondrodysplasia punctata (CDPX) and implications for warfarin embryopathy. *Cell* 81: 15–25.
13. Ogata T, Matsuo N (1993) Sex chromosome aberrations and stature: deduction of the principal factors involved in the determination of adult height. *Hum Genet* 91: 551–562.
14. Rao E, Weiss B, Fukami M, Rump A, Niesler B, et al. (1997) Pseudoautosomal deletions encompassing a novel homeobox gene cause growth failure in idiopathic short stature and Turner syndrome. *Nat Genet* 16: 54–63.
15. Ogata T, Matsuo N (1995) Turner syndrome and female sex chromosome aberrations: deduction of the principal factors involved in the development of clinical features. *Hum Genet* 95: 607–629.
16. Ogata T, Muroya K, Matsuo N, Shinohara O, Yorifuji T, et al. (2001) Turner syndrome and Xp deletions: clinical and molecular studies in 47 patients. *J Clin Endocrinol Metab* 86: 5498–5508.
17. Ogata T, Tyler-Smith C, Purvis-Smith S, Turner G (1993) Chromosomal localisation of a gene(s) for Turner stigmata on Yp. *J Med Genet* 30:918–922.